ORIGINAL RESEARCH

PDE8 Is Expressed in Human Airway Smooth Muscle and Selectively Regulates cAMP Signaling by β_2-Adrenergic Receptors and Adenylyl Cyclase 6

Timothy B. Johnstone[1], Kaitlyn H. Smith[2], Cynthia J. Koziol-White[3], Fengying Li[2], Austin G. Kazarian[1], Maia L. Corpuz[1], Maya Shumyatcher[4], Frederick J. Ehlert[5], Blanca E. Himes[4], Reynold A. Panettieri, Jr.[3], and Rennolds S. Ostrom[1]

[1]Department of Biomedical and Pharmaceutical Sciences, Chapman University School of Pharmacy, Irvine, California; [2]Department of Pharmacology, University of Tennessee Health Science Center, Memphis, Tennessee; [3]Rutgers Institute for Translational Medicine and Science, Child Health Institute, Rutgers University, New Brunswick, New Jersey; [4]Department of Biostatistics, Epidemiology and Informatics, University of Pennsylvania, Philadelphia, Pennsylvania; and [5]Department of Pharmacology, School of Medicine, University of California, Irvine, Irvine, California

Abstract

Two cAMP signaling compartments centered on adenylyl cyclase (AC) exist in human airway smooth muscle (HASM) cells, one containing β_2-adrenergic receptor AC6 and another containing E prostanoid receptor AC2. We hypothesized that different PDE isozymes selectively regulate cAMP signaling in each compartment. According to RNA-sequencing data, 18 of 24 PDE genes were expressed in primary HASM cells derived from age- and sex-matched donors with and without asthma. *PDE8A* was the third most abundant of the cAMP-degrading PDE genes, after *PDE4A* and *PDE1A*. Knockdown of PDE8A using shRNA evoked twofold greater cAMP responses to 1 μM forskolin in the presence of 3-isobutyl-1-methylxanthine. Overexpression of AC2 did not alter this response, but overexpression of AC6 increased cAMP responses an additional 80%. We examined cAMP dynamics in live HASM cells using a fluorescence sensor. PF-04957325, a PDE8-selective inhibitor, increased basal cAMP concentrations by itself, indicating a significant basal level of cAMP synthesis. In the presence of an AC inhibitor to reduce basal signaling, PF-04957325 accelerated cAMP production and increased the inhibition of cell proliferation induced by isoproterenol, but it had no effect on cAMP concentrations or cell proliferation regulated by prostaglandin E_2. Lipid raft fractionation of HASM cells revealed PDE8A immunoreactivity in buoyant fractions containing caveolin-1 and AC5/6 immunoreactivity. Thus, PDE8 is expressed in lipid rafts of HASM cells, where it specifically regulates β_2-adrenergic receptor AC6 signaling without effects on signaling by the E prostanoid receptors 2/4–AC2 complex. In airway diseases such as asthma and chronic obstructive pulmonary disease, PDE8 may represent a novel therapeutic target to modulate HASM responsiveness and airway remodeling.

Keywords: cAMP compartmentation; PDE; lipid rafts; adenylyl cyclase

Clinical Relevance

The findings we present establish a new potential target for regulating bronchodilators in asthma or chronic obstructive pulmonary disease. PDE8 is a less widely expressed form of PDE and specifically regulates β-adrenergic receptor–mediated bronchodilators. These features may provide an advantaged therapeutic profile for PDE8 inhibition.

(Received in original form August 19, 2017; accepted in final form December 20, 2017)

Supported by the National Institutes of Health (NIH) through National Institute of General Medical Sciences grant GM107094.

Author Contributions: Conception and design: T.B.J., F.J.E., B.E.H., R.A.P., and R.S.O.; conducted experiments: T.B.J., K.H.S., C.J.K.-W., F.L., A.G.K., M.L.C., M.S., B.E.H., and R.S.O.; analysis and interpretation: T.B.J., K.H.S., C.J.K.-W., M.S., F.J.E., B.E.H., R.A.P., and R.S.O.; and drafting the manuscript for important intellectual content: T.B.J., K.H.S., C.J.K.-W., F.J.E., B.E.H., R.A.P., and R.S.O.

Correspondence and requests for reprints should be addressed to Rennolds S. Ostrom, Ph.D., Department of Biomedical and Pharmaceutical Sciences, Chapman University School of Pharmacy, 9501 Jeronimo Road, Irvine, CA 92618. E-mail: rostrom@chapman.edu.

This article has a data supplement, which is accessible from this issue's table of contents at www.atsjournals.org.

Am J Respir Cell Mol Biol Vol 58, Iss 4, pp 530–541, Apr 2018

Originally Published in Press as DOI: 10.1165/rcmb.2017-0294OC on December 20, 2017
Internet address: www.atsjournals.org

Human airway smooth muscle (HASM) hypercontractility in asthma and chronic obstructive pulmonary disease (COPD) has long been managed through the use of short-acting and long-acting β_2-adrenergic receptor (β_2AR) agonists. Protein kinase A (PKA) activation by cAMP is a key step in bronchodilation (1); thus, defining the elements responsible for cAMP signal termination is critical. Many G protein–coupled receptors (GPCRs) expressed in HASM cells use cAMP signaling as their main second messenger, but agonists for these receptors elicit different responses. This phenomenon supports the widely held belief that cAMP signaling is compartmentalized (2, 3); yet, little is known about how cells accomplish this compartmentation (4). Cells require discrete signaling elements to convey both spatial and temporal cAMP dynamics to selectively and finely tune propagated responses. GPCRs selectively organize the initial response from paracrine, hormonal, or transmitter effectors to modulate subsequent intracellular changes in cAMP concentrations by coupling through G_s and/or G_i proteins (5, 6). Adenylyl cyclases (ACs) produce cAMP, but they also assemble selective responses based on AC isoform–specific stratification to raft or nonraft microdomains, proximity to associated GPCRs, and scaffolding of associated proteins and enzymes to create distinct signalosomes (4, 7). Two principal cAMP signaling compartments have been defined in HASM, one consisting of β_2ARs coupled to AC6 and another of E prostanoid 2/4 receptors ($EP_{2/4}$Rs) coupled exclusively to AC2 (8–11). This cAMP "circuitry" is a dynamic and dimensional network that decodes similar, context-specific cAMP signals from different GPCRs and integrates the input for membrane, cytosolic, or nuclear output targets within the cell.

PDEs terminate cAMP signals by catalyzing the conversion of cAMP into 5′-AMP and regulate the duration and magnitude of signaling at localized complexes to provide spatial regulation (12). These properties confer a distinct role for PDEs to sculpt the circuitry by shaping the strength and intracellular direction of the cAMP signal (3). PDEs influence signal gain, or the sensitivity of output relative to degree of input. PDEs also regulate the sensitivity of cAMP pathways by participating as negative feedback regulators of cell signaling, because PDE upregulation ensures that additional signaling will not produce a cellular response until a higher stimulus threshold is reached (13–15). A-kinase–anchoring proteins play a central role in tethering PKA to PDE to facilitate this negative feedback (16). PDEs constitute a superfamily of 24 genes that are classified into 11 gene families (PDE1–PDE11) according to their N-terminal domains. Different cell types orchestrate PDE activity in cells by expressing a unique complement of PDE genes depending on the spatial and kinetic requirements for cAMP signaling (12). Thus, the potential to selectively modulate cAMP signaling at the PDE level is significant, but little is known about how different PDE isozymes localize to cAMP signalosomes (2, 3).

Inhibition of PDE4 augments β-agonist relaxation of smooth muscle cells and promotes bronchodilation (17, 18). However, PDE4 control exerted over β_2AR signaling appears to be broad (19). PDE4 inhibitors have nonselective and indiscriminate effects in many tissues, limiting their therapeutic utility (20, 21). PDE8 may selectively modulate β_2AR signaling with fewer side effects: It has higher affinity and lower K_m for cAMP than other PDE isoforms to shape low-level, highly localized cAMP signals (22, 23). Cardiac myocytes of *PDE8A*-knockout mice display higher Ca^{2+} transients, greater basal Ca^{2+} spark frequency and increased L-type calcium channel current after isoproterenol stimulation (24). These reflect changes in basal settings that occur without induction of global PKA activity and may indicate compartment-specific control by PDE8.

In the present study, we sought to define the PDE isozymes expressed in HASM cells, with the goal of determining if specific PDEs participate in previously defined cAMP signaling compartments (8, 10). Our studies indicate that a less widely expressed isoform of PDE, *PDE8A*, is expressed in HASM cells. We present a possible role of PDE8 in these cells using specific PDE8 inhibitors and shRNA knockdown of PDE8A expression. Our findings are consistent with the idea that PDE8A localizes in lipid raft microdomains, where its activity shapes responses to colocalized β_2AR-AC6 signals without altering AC2 signaling by E prostanoid receptors localized in nonraft microdomains. Some of the results of these studies were previously reported in the form of an abstract (25).

Methods

Materials

Forskolin was purchased from LC Laboratories. PF-04957325 was a generous gift from Pfizer, Inc. Cell culture media and components were purchased from Thermo Fisher Scientific. FBS was purchased from Atlanta Biologicals. Lentiviral particles expressing PDE8A shRNA were purchased from Santa Cruz Biotechnology. Secondary antibodies were obtained from Santa Cruz Biotechnology. All other drugs and chemicals were purchased from Sigma-Aldrich unless otherwise noted.

Cell Culture

HASM cells were isolated from deceased, de-identified lung donors by enzymatic dissociation in accordance with institutional review board approval and as described previously (26). HASM cells were grown in Ham's F-12 media supplemented with 10% FBS, penicillin-streptomycin, 25 mM HEPES, 1.7 mM $CaCl_2$, and L-glutamine. Cells were kept at 5% CO_2 and 37°C. Experiments were performed on cells from passages 3–7 using over 20 different primary cell isolates in total and in at least 3 different isolates for each study. Adenoviral constructs expressing AC2, AC6, or lacZ (control) cDNA were used in AC overexpression studies. The titer of AC virus was chosen to give similar global cAMP concentrations in response to 1 μM forskolin. Cells were infected 18 hours before treatment.

RNA Sequencing

We obtained RNA-sequencing (RNA-Seq) results from a previously published study for transcripts of all known PDE genes (27). Briefly, primary airway smooth muscle (ASM) cells were isolated from 10 white nonsmoking donors with no chronic illness or medication use and from 5 white donors with asthma. ASM cell cultivation was described previously (26, 28). Passages 4–7 ASM cells maintained in Ham's F-12 medium supplemented with 10% FBS and $CaCl_2$ and buffered with HEPES, penicillin-streptomycin, primocin, and additional L-glutamine were used in all experiments. The F-12 medium was used for culture because it provides Ca^{2+} concentrations

that enable visualization of the contractility of muscles in that medium. Total RNA was extracted from cells using the miRNeasy Mini Kit (Qiagen Sciences, Inc.). Approximately 1 μg of RNA from each sample was used to generate RNA-Seq cDNA libraries for sequencing using the TruSeq RNA Sample Prep Kit v2 (Illumina, Inc.). Sequencing of 75-bp paired-end reads was performed with an Illumina HiSequation 2000 instrument at Partners Personalized Medicine. taffeta scripts (https://github.com/blancahimes/taffeta) were used to analyze RNA-Seq data, which included using trimmomatic (v.0.32) (29) for trimming of adapters and FastQC (v.0.11.2; Babraham Bioinformatics) to obtain overall QC metrics. kallisto software was used to estimate transcript counts according to the hg38 Ensembl reference human genome (30). Sleuth software was used to test for differential expression of transcripts between donors with and without asthma (31). Transcripts were considered to be expressed if at least 47% of samples had five or more reads. Plots were made with R software (2017; R Development Core Team, R Foundation for Statistical Computing). RNA-Seq data are available in the Gene Expression Omnibus under accession number [GEO:GSE58434].

cAMP Assays

For endpoint studies, HASM cells were grown to 80% confluency on 24-well plates, washed once with serum- and $NaHCO_3$-free Dulbecco's modified Eagle's medium supplemented with 20 mM HEPES, pH 7.4, then equilibrated for 30 minutes in a 37°C water bath. In most studies, cells were pretreated with 0.2 mM 3-isobutyl-1-methylxanthine (IBMX, a broad-spectrum PDE inhibitor), then exposed to the indicated drug for 15 minutes. In other studies, no IBMX was included, and the assay incubation time was 7 minutes. Assay medium was aspirated at the end of the incubation period, and 30 μl of lysis buffer was added to each well to terminate the reaction. cAMP content was then assayed using the HitHunter cAMP Assay for Small Molecules Kit (DiscoverX). Data were normalized to the average amount of total protein on each plate as determined using a dye-binding protein assay (Bio-Rad Laboratories).

For kinetic measurement of cAMP production in live cells, subconfluent HASM cells were plated on a black-walled, clear, flat-bottomed 96-well plate with 100 μl of HASM cell media, 40 μl of baculovirus modified with a mammalian promoter expressing the green cAMP difference detector *in situ* (cADDis) cAMP sensor (Montana Molecular), and 1 μM trichostatin A (Sigma-Aldrich) per well. Cells were grown overnight at 5% CO_2 and 37°C. Media were aspirated and replaced with 180 μl per well of 1× Dulbecco's PBS solution without calcium and magnesium. The 96-well plate was covered with aluminum foil and incubated at room temperature for 30 minutes. Cell fluorescence was read from the plate bottom using excitation/emission wavelengths of 494 nm and 522 nm, respectively, with a SpectraMax M5 plate reader (Molecular Devices). A 5-minute kinetic read on unstimulated cells was performed to determine if the variability in each well's fluorescence was less than or equal to 5%. Cells were stimulated with agonist and/or PDE inhibitor, and fluorescence changes in each well were read at 30-second intervals for 30 minutes. Data were fit to a single-site decay model using Prism 6.0 software (GraphPad Software Inc.). In some cases, the kinetic rate constant (k) was compared between treatments by constraining the curve fits to a common plateau and plotting k to compare the rate of cAMP production across different treatments.

For assays of AC activity, membranes from HASM cells were prepared by scraping cells into a hypotonic homogenizing buffer (30 mM Na-HEPES, 5 mM $MgCl_2$, 1 mM EGTA, 2 mM DTT, pH 7.5) and homogenizing them in a Dounce homogenizer. The homogenate was spun at 300 × g for 5 minutes at 4°C, then transferred to a new tube and spun at 5,000 × g for 10 minutes. The pellet was suspended in membrane buffer (30 mM Na-HEPES, 5 mM $MgCl_2$, 2 mM DTT, pH 7.5) to yield a 1 mg/ml total protein concentration. A quantity of 30 μl of membranes was added to assay buffer (30 mM Na-HEPES, 100 mM NaCl, 1 mM EGTA, 10 mM $MgCl_2$, 1 mM IBMX, 1 mM ATP, 10 mM phosphocreatine, 5 μM GTP, 60 U/ml creatine phosphokinase, 0.1% BSA, pH 7.5) and either 1 μM forskolin or 10 μM SQ22536 or both. Reactions were run for 15 minutes at 30°C, then stopped by boiling for 5 minutes. Each tube was assayed for cAMP content using the HitHunter cAMP Assay for Small Molecules Kit. Total protein concentration was determined using a dye-binding protein assay (Bio-Rad Laboratories).

Nondetergent Isolation of Lipid Raft and Nonraft Membranes

Cells were fractionated using a detergent-free method as previously described (8). HASM cells were grown to 70 to 80% confluency on 10-cm plates. Cells were washed twice in ice-cold PBS, scraped off the plate in 500 mM sodium carbonate, pH 11, and then homogenized with 20 strokes in a glass-glass tissue grinder followed by three 20-second bursts with an ultrasonic cell disruptor. An equal volume of 90% sucrose in 2-(*N*-morpholino) ethanesulfonic acid–buffered saline (25 mM 2-[*N*-morpholino]ethanesulfonic acid and 150 mM NaCl, pH 6.5) was added. The sample was loaded at the bottom of a discontinuous sucrose gradient of 35% and 5% sucrose (prepared in 2-[*N*-morpholino] ethanesulfonic acid–buffered saline with 250 mM Na_2CO_3). The gradient was centrifuged at 46,000 rpm on a SW 55 Ti rotor (Beckman Coulter) for 18 hours at 4°C. Fractions (500 ml each) were collected from the top of the gradient and then analyzed by SDS-PAGE (loading equal proportions of each fraction) and immunoblotting. For AC isoform detection, samples were deglycosylated and concentrated before SDS-PAGE. Protein (80–100 μg) was incubated with peptide:N-glycosidase F in 60 mM NaCl, 1.25 mM EDTA, 143 mM β-mercaptoethanol, 5 mM sodium phosphate, 15 mM Tris-HCl (pH 7.5), 0.1% SDS, and 0.5% Nonidet P-40 for 2 hours at 37°C. Reactions were terminated with 0.33 volumes of 4× SDS-PAGE sample buffer.

Immunoblot Analysis

Whole-cell lysates were obtained by scraping cells in modified radioimmunoprecipitation assay lysis buffer (50 mM Tris-HCl, pH 7.5, 150 mM NaCl, 1% IGEPAL CA-630, plus mammalian protease inhibitor cocktail [catalogue number P-8340; Sigma-Aldrich]) and homogenizing them by sonication. Whole-cell lysates or cell fractions were separated on 10% SDS-polyacrylamide gels by electrophoresis before being transferred to polyvinylidene fluoride membranes (EMD Millipore) by electroblotting. Membranes were blocked in 20 mM PBS with 3% nonfat dry milk and incubated with primary antibody for

2–12 hours at 4°C with constant rocking. PDE8A antibody (catalogue number sc-17232; 1:200 dilution), β-actin antibody (catalogue number sc-47778; 1:1,000 dilution), AC2 antibody (catalogue number sc-587; 1:200 dilution), and AC5/6 antibody (catalogue number sc-590; 1:200 dilution) were obtained from Santa Cruz Biotechnology. Caveolin-1 monoclonal antibody (catalogue number 610057, 1:1,000 dilution) was obtained from BD Biosciences. Bound primary antibodies were visualized using appropriate secondary antibody with conjugated horseradish peroxidase (Santa Cruz Biotechnology) and enhanced chemiluminescence reagent (Thermo Fisher Scientific). Images were captured using the Bio-Rad Gel Doc System, then the alignment, exposure, and contrast of each image was optimized using Adobe Photoshop Creative Suite 4 software. In some cases, immunoreactive bands were evaluated by densitometric analysis using the volume plus density method and normalized to β-actin.

Cell Proliferation Assay

HASM cells were plated on 96-well plates at a density of 5,000 cells per well. After attachment, media were changed to serum-free conditions (Ham's F-12 supplemented with 1% insulin-transferrin-selenium [Sigma-Aldrich], penicillin-streptomycin, 25 mM HEPES, 1.7 mM $CaCl_2$, and L-glutamine). After 48 hours, the indicated drugs with or without 10% FBS were added. After another 48 hours, the total cell content of each well was measured using the CyQUANT NF Cell Proliferation Assay Kit (Thermo Fisher Scientific) according to the manufacturer's instructions.

Data Analysis and Statistics

Standard curves were fit, and unknown values were extrapolated using Prism 6.0 software. Data are presented as the mean ± SEM. Statistical comparisons (*t* tests and one-way ANOVA) were performed, and figures were generated using Prism 6.0 software.

Results

To understand how cAMP signaling is regulated in HASM cells, we characterized the isozymes responsible for cAMP catabolism. Transcript measurements for all PDE genes were performed in HASM cells derived from age- and sex-matched donors with and without asthma using RNA-Seq. Fifty-five transcripts corresponding to 18 different PDE genes were expressed, whereas 6 PDE genes (*PDE1B*, *PDE2A*, *PDE6A*, *PDE6C*, *PDE6G*, and *PDE6H*) did not have expressed transcripts (Table 1). Box plots showing expression levels in cells derived from donors with versus donors without asthma for the 12 most abundant PDE gene transcripts are shown in Figure 1. None of the transcripts were differentially expressed between donors with and without asthma according to false discovery rate–corrected statistics, although *PDE4A* had nominally significant results for its most abundant transcript (ENST00000380702; $P = 0.034$). Among the PDE isoforms that hydrolyze cAMP, *PDE8A* was the third most abundant transcript (following *PDE1A* and *PDE4A* and roughly equivalent to *PDE7A*) (Table 1). No previous reports have demonstrated expression of this PDE isoform in lung tissue or smooth muscle cells of any origin.

PDE8A is an IBMX-insensitive isoform that is not widely expressed in peripheral cells and tissues. Because PDE8 is not inhibited by most broad-spectrum PDE inhibitors (32), we wondered if previous studies of cAMP signaling in HASM had failed to account for activity of this PDE. We measured cAMP production in HASM cells from normal donors in the presence of 0.2 mM IBMX (to reduce activity by most other PDE isoforms) with and without dipyridamole, a PDE5/PDE8 inhibitor (22, 32–34). Basal cAMP production in lacZ controls showed no increase in cAMP production when we used 30 μM dipyridamole compared with vehicle control (Figure 2A). We also overexpressed either AC2 or AC6, two isoforms natively expressed in HASM cells (8), to determine if increased cAMP synthesis revealed a role for PDE8A activity in either the AC2 or AC6 signaling compartments. Dipyridamole had no effect on basal cAMP concentrations in AC2-overexpressing HASM cells, but a small, nonsignificant increase in basal cAMP production was evident in AC6-overexpressing cells. When cells were stimulated with 1 μM forskolin, we observed a significant increase in cAMP concentrations in AC6-overexpressing HASM cells but no significant effect in the lacZ- or AC2-overexpressing cells (Figure 2B).

Dipyridamole has been reported to also inhibit multidrug resistance-associated protein 4, a transport channel that pumps

Table 1. PDE Genes Expressed in Human Airway Smooth Muscle Cells Derived from Donors with and without Asthma

Gene	Transcript	Observed Reads Mean (Variance)	Transcripts per Million Mean (SD)
PDE1A	ENST00000351439	6.00 (0.32)	8.75 (5.13)
PDE1C	ENST00000396184	5.56 (0.70)	1.63 (1.32)
PDE3A	ENST00000359062	5.24 (0.45)	1.27 (0.93)
PDE3B	ENST00000282096	6.26 (0.22)	3.89 (1.73)
PDE4A	ENST00000380702	7.22 (0.02)	11.96 (1.50)
PDE4B	ENST00000371045	5.12 (0.90)	2.55 (2.30)
PDE4C	ENST00000355502	3.57 (0.25)	0.27 (0.14)
PDE4D	ENST00000546160	5.08 (0.54)	1.05 (0.65)
PDE5A	ENST00000394439	9.18 (0.12)	62.61 (22.49)
PDE6B	ENST00000496514	2.34 (1.30)	0.19 (0.13)
PDE6D	ENST00000287600	6.29 (0.02)	21.61 (2.49)
PDE7A	ENST00000401827	5.89 (0.04)	4.21 (0.77)
PDE7B	ENST00000308191	5.26 (0.08)	1.53 (0.48)
PDE8A	ENST00000310298	5.92 (0.16)	4.18 (1.57)
PDE8B	ENST00000264917	4.28 (0.16)	0.54 (0.23)
PDE9A	ENST00000335512	1.45 (2.86)	0.25 (0.29)
PDE10A	ENST00000366882	3.48 (2.25)	0.30 (0.29)
PDE11A	ENST00000286063	1.55 (1.62)	0.03 (0.03)

Human airway smooth muscle cells were derived from 5 donors with asthma and 10 donors without asthma. The mean number of observed reads across all samples and its variance are shown for the most abundant transcript of the corresponding PDE gene. Also shown for these transcripts are the mean and SD of the transcripts per million, a normalized estimate of transcript expression obtained with the kallisto software program. Six PDE genes (*PDE1B*, *PDE2A*, *PDE6A*, *PDE6C*, *PDE6G*, and *PDE6H*) were not expressed (i.e., did not have ⩾47% of samples with five or more observed reads).

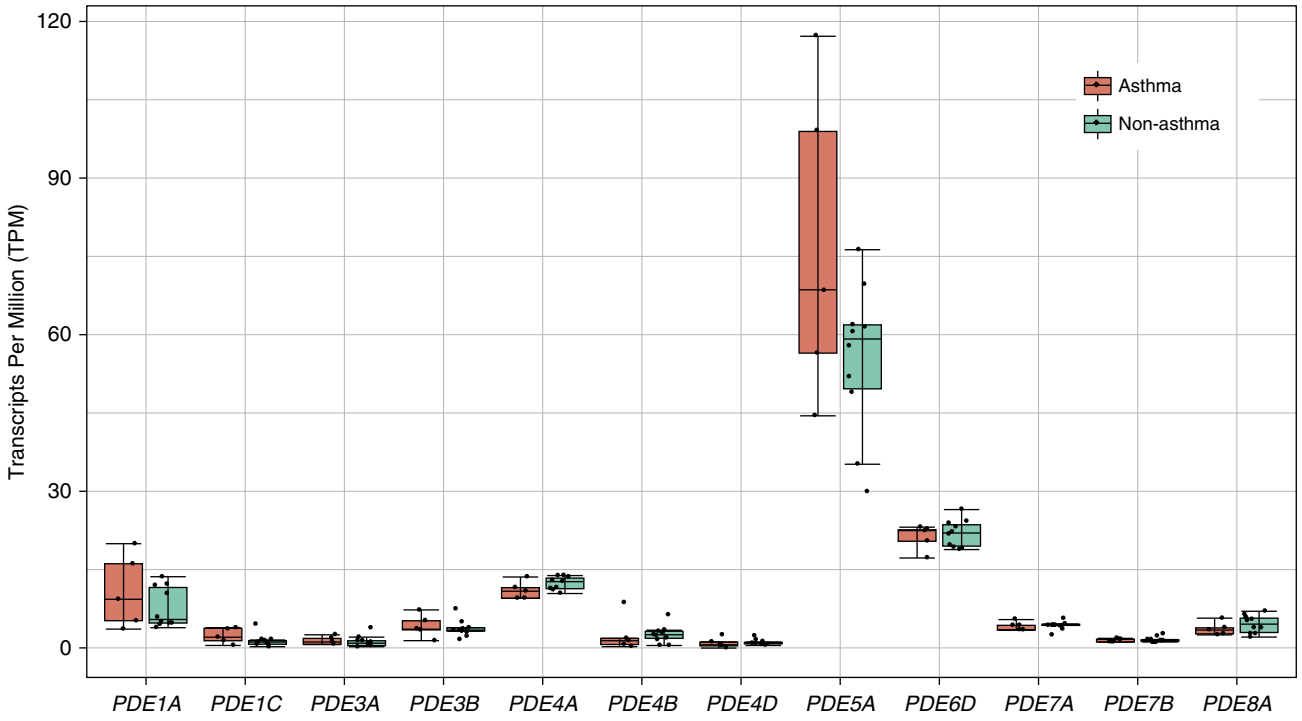

Figure 1. Box plots of transcripts per million for the most highly expressed transcript of each PDE gene that had mean observed counts greater than 5. Data were obtained from RNA-sequencing results of human airway smooth muscle cells derived from age- and sex-matched donors with fatal asthma ($n = 5$) and without asthma ($n = 10$). Transcript count estimates were obtained using kallisto software with the hg38 Ensembl human genome as a reference.

cAMP out of cells (35). The observed changes shown in Figure 2 may have been confounded by altered cAMP export, because the assay we used detected only intracellular cAMP. To attain a more specific reduction in PDE8A activity, we used shRNA to knock down its expression. We tested a commercially available PDE8A shRNA lentiviral vector at different viral titers and treatment times to determine the optimal conditions for knockdown of PDE8A. We detected a maximal reduction in PDE8A immunoreactivity in lacZ- (control), AC2-, and AC6-overexpressing HASM cells (Figures 3A and 3B) 4 days after infection with PDE8A shRNA lentivirus. In the presence of IBMX, basal cAMP production was not significantly different between HASM cells infected with scrambled (control) lentivirus and those infected with PDE8A shRNA (Figure 3C). However, when AC activity was stimulated with 1 μM forskolin, PDE8A knockdown increased cAMP accumulation in control HASM cells and cells overexpressing AC6 (Figure 3D). By contrast, PDE8A knockdown did not significantly increase

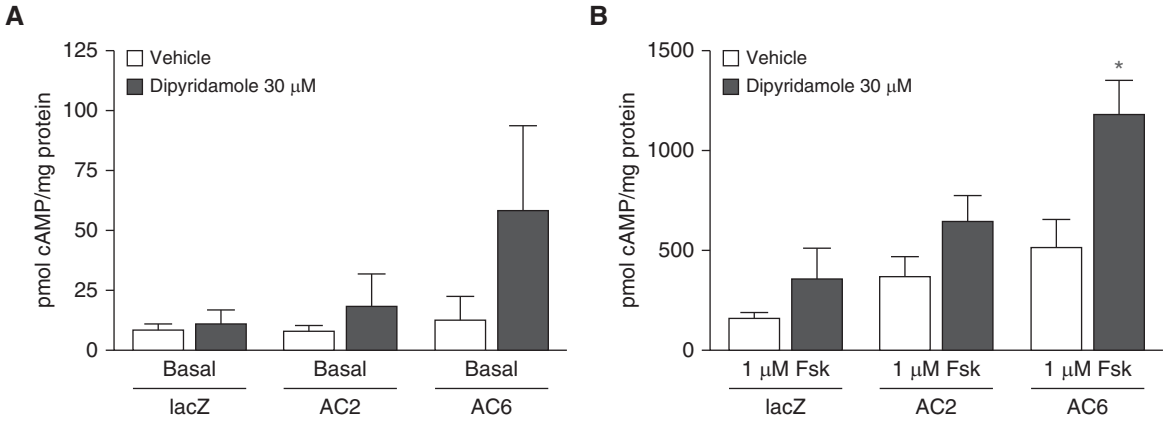

Figure 2. The effect of 30 μM dipyridamole on cAMP accumulation in human airway smooth muscle cells in (*A*) basal conditions or (*B*) 1 μM forskolin (Fsk)-stimulated conditions. Human airway smooth muscle cells were incubated with recombinant adenoviruses expressing either lacZ, adenylyl cyclase 2 (AC2), or AC6 for 18 hours. cAMP accumulation was then measured over 10 minutes in the presence of 200 μM 3-isobutyl-1-methylxanthine. Data are expressed as the mean ± SEM ($n = 5$ experiments). *$P < 0.05$ by paired *t* test compared with vehicle.

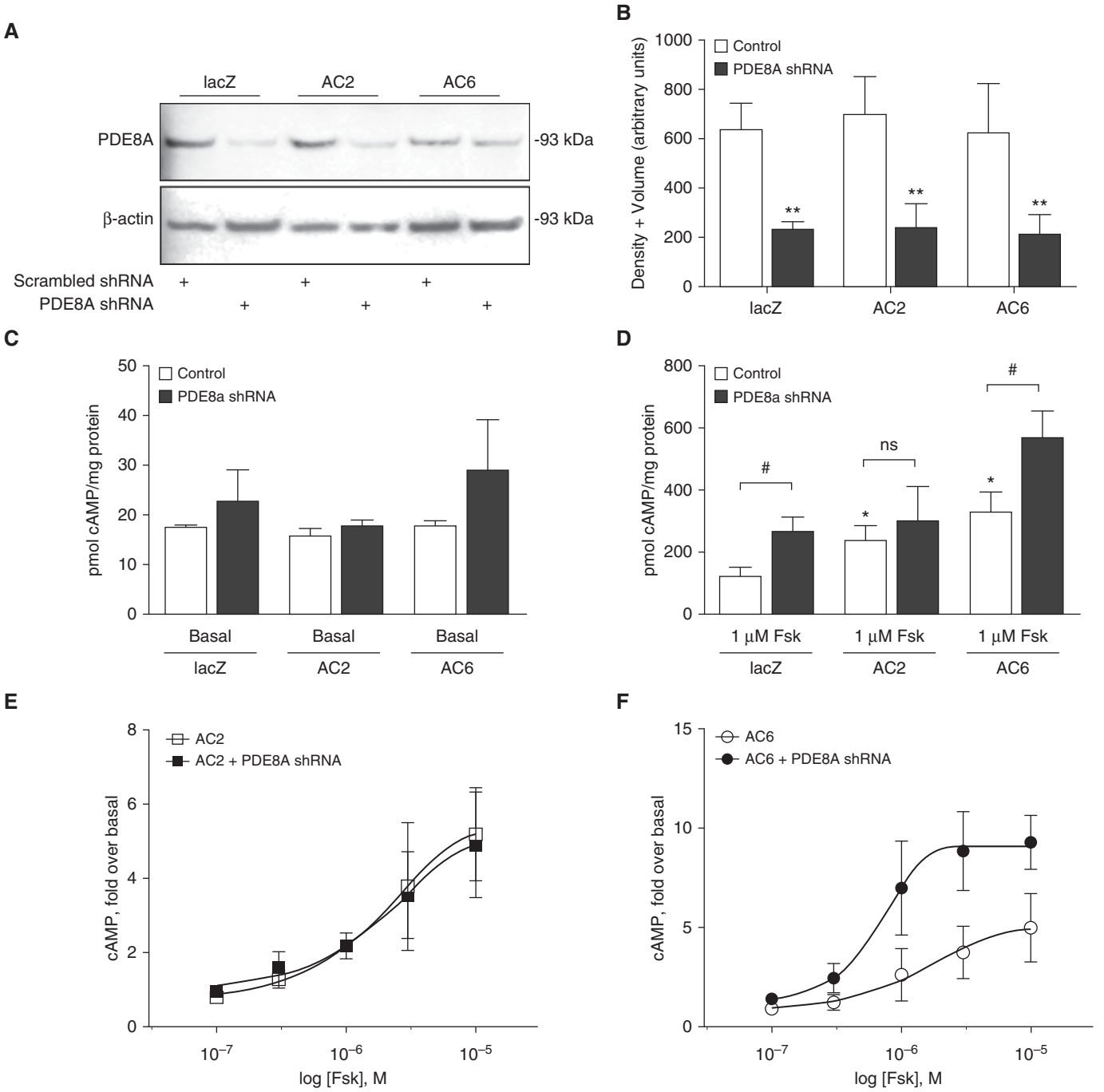

Figure 3. PDE8A knockdown in human airway smooth muscle (HASM) cells. (*A*) Immunoblot analysis of PDE8A and β-actin in HASM cells after 72-hour incubation with recombinant lentivirus expressing scrambled or PDE8A shRNA. The PDE8A antibody detected multiple nonspecific bands. The genuine PDE8A immunoreactivity was identified on the basis of the expected molecular weight of 93 kD, so only this band is shown (representative images of $n = 3$ experiments are shown). Full immunoblot of PDE8A is shown in Figure E1. (*B*) Immunoreactive bands were analyzed by densitometry using volume plus density, and PDE8A density was normalized to the β-actin loading control. Data are expressed as the mean ± SEM ($n = 3$ experiments). $^{**}P < 0.01$ by paired *t* test as compared with control. The effect of PDE8A knockdown on cAMP accumulation in HASM cells in (*C*) basal or (*D*) 1 μM Fsk-stimulated conditions. HASM cells were incubated with recombinant lentivirus expressing scrambled or PDE8A shRNA for 72 hours and recombinant adenoviruses expressing either lacZ, AC2, or AC6 for 18 hours. cAMP accumulation was measured over 10 minutes in the presence of 200 μM 3-isobutyl-1-methylxanthine. Data are expressed as the mean ± SEM ($n = 5$ experiments). $^{*}P < 0.05$ by paired *t* test as compared with lacZ; $^{\#}P < 0.05$ by paired *t* test as compared with control. cAMP stimulated by various concentrations of forskolin was measured in HASM cells overexpressing either (*E*) AC2 or (*F*) AC6. Data are expressed as the mean ± SEM ($n = 4$ experiments). Nonlinear regression analysis was used to fit each dataset. The logarithmic half-maximal effective concentration for forskolin in AC6 cells was −4.97 ± 0.232 M, and the maximal effect value was 4.96 ± 0.785 fold. The logarithmic half-maximal effective concentration for forskolin in AC6 cells treated with PDE8A shRNA was −6.24 ± 0.481 M, and the maximal effect value was 9.069 ± 0.609 fold. ns = not significant.

cAMP accumulation in HASM cells overexpressing AC2 (Figure 3D).

We next measured cAMP production across a range of forskolin concentrations. The concentration–response curves for forskolin in the absence and presence of PDE8A knockdown were superimposable in AC2-overexpressing HASM cells (Figure 3E). In AC6-overexpressing HASM cells, both the half-maximal effective concentration and maximal effect of forskolin-stimulated cAMP production were enhanced in PDE8A-knockdown cells (Figure 3F). These data are consistent with the idea that PDE8A catalyzes the degradation of cAMP in the AC6 compartment with little effect on cAMP synthesized by AC2.

β_2AR can couple primarily to AC6, whereas $EP_{2/4}R$ couples only to AC2, owing to the colocalization of these GPCRs with their respective AC isoforms (9). We hypothesized that β_2AR-mediated signaling in HASM cells is selectively regulated by PDE8A activity. To test this idea, we examined cAMP production using cADDis, a fluorescent sensor that detects cytosolic cAMP concentrations in live cells (36). Preliminary studies demonstrated that we could observe large decreases in fluorescence of the downward cADDis sensor in response to various concentrations of forskolin without the addition of IBMX or other PDE inhibitors (Figure 4A). Addition of PF-04957325, a PDE8-selective inhibitor (37), also increased concentrations of cAMP in a concentration-dependent manner (Figures 4B and 4E). We observed a similar response with the addition of rolipram, a PDE4-selective inhibitor (Figure 4C), implying that a low level of basal AC activity exists in HASM cells. This basal AC activity is sufficient to allow PDE inhibition alone to induce cAMP responses detected by the cADDis sensor.

To use PF-04957325 to probe for the role of PDE8 in regulating cAMP stimulated by isoproterenol or prostaglandin E_2 (PGE_2), this basal AC activity must be reduced. This is a critical element, because the source of the basal stimulus, as well as the compartment(s) and AC isoform(s) from which it emanates, is unknown. We sought an established AC inhibitor that is relatively nonselective across AC

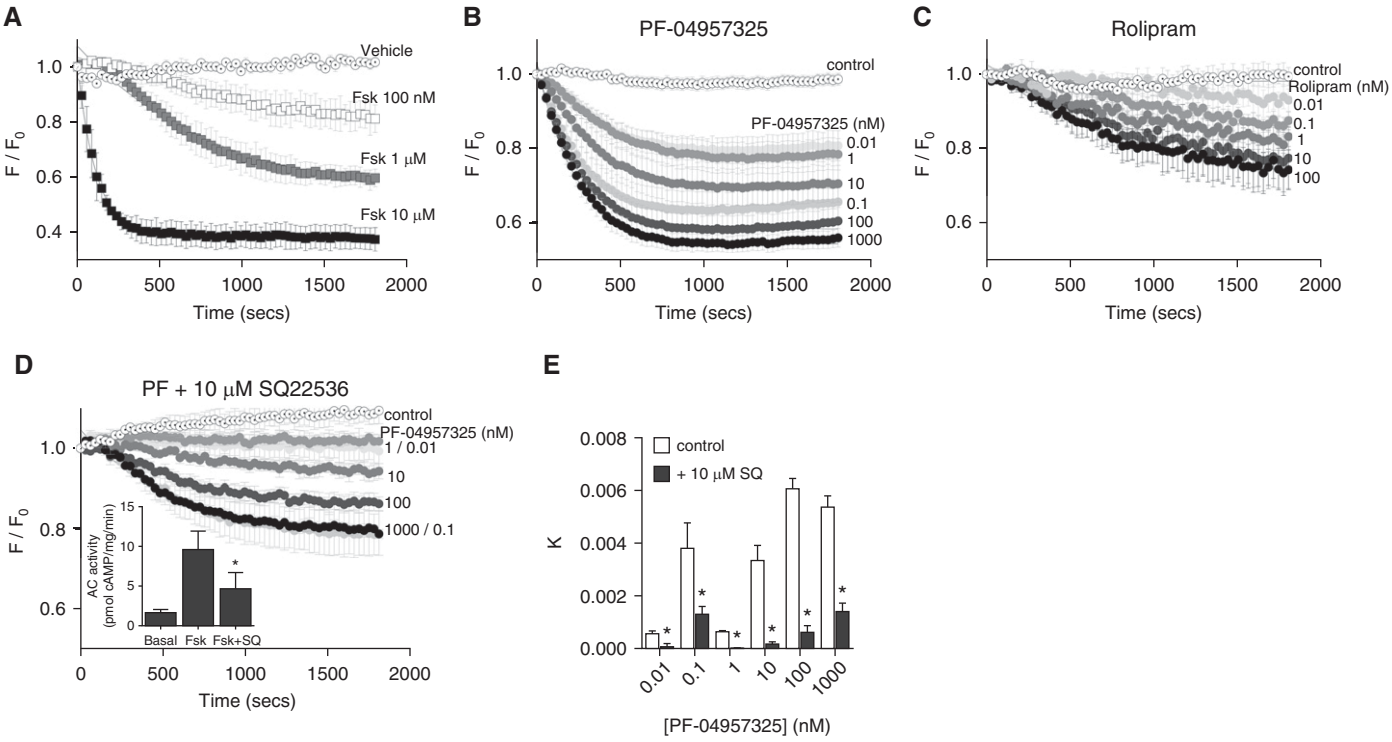

Figure 4. cAMP dynamics in live HASM cells measured using the cAMP difference detector *in situ* (cADDis) assay. HASM cells were incubated with recombinant baculovirus modified with a mammalian promoter expressing the cADDis cAMP sensor for 24 hours. After baseline values were established, fluorescence decay was monitored for 30 minutes after addition of the indicated agent. cADDis sensor fluorescence decay curves elicited by various concentrations of (*A*) Fsk, (*B*) PF-04957325, or (*C*) rolipram are shown, with each point representing the mean ± SEM ($n = 3$–5 experiments). (*D*) Responses to the same concentrations of PF-04957325 were measured in the presence of 10 μM SQ22536 to reduce basal cAMP synthesis. The ability of SQ22536 to inhibit adenylyl cyclase activity was confirmed in HASM membranes stimulated with 1 μM forskolin or forskolin plus 10 μM SQ22536 (*D*, inset). PF-04957325 was tested at concentrations from 10^{-11} M (lightest filled circle) to 10^{-6} M (black filled circle). Control (vehicle) responses are plotted as dotted open circles, and 10 μM forskolin is plotted as dotted open squares. Data are gathered as arbitrary fluorescence units and expressed as observed fluorescence (F) over initial fluorescence (F_0) to indicate fluorescence remaining after stimulation. SQ22536 (10 μM) was added 5 minutes before initiating a 30-minute read with PF-04957325. (*E*) Kinetic rate constants (*k*) were derived from a shared constrained plateau of one-phase decay analysis among the control and the doses of PF-04957325 with constrained Hill slope of 2 and plotted. The logarithmic half-maximal effective concentration for PF-04957325 alone was determined to be −8.034 ± 0.193 M, and the maximal effect value for the span of *k* was 0.00516 ± 0.00118. The logarithmic half-maximal effective concentration for PF-04957325 with 10 μM SQ22536 was determined to be −6.921 ± 0.339 M, and the maximal effect value for the span of *k* was 0.001341 ± 0.0005293. Each bar represents the mean ± SEM ($n = 5$ experiments). *$P < 0.05$ by paired *t* test as compared with control.

isoforms. We tested several concentrations of the AC inhibitor SQ22536 (38) to find the minimally effective concentration that reduces the cAMP response to PF-04957325 alone. At 10 μM concentration, SQ22536 caused a significant reduction in the observed responses to PF-04957325 (Figures 4D and 4E). This same concentration of SQ22536 reduced AC activity in isolated HASM membranes by about 50% (Figure 4D, inset). Using 10 μM SQ22536 to suppress basal AC activity, various concentrations of isoproterenol or PGE_2 were used to identify concentrations of each agonist that induced small but reproducible cAMP stimuli of equal magnitude. Isoproterenol (1 nM) or PGE_2 (3 nM), each of which elicits half-maximal responses by the cADDis sensor when tested alone, produced an approximately 5 to 10% reduction of the fluorescent signal in the presence of 10 μM SQ22536 (Figure 5A). We then measured the responses to various concentrations of PF-04957325 in the presence of 10 μM SQ22536 with either isoproterenol or PGE_2 present to provide compartment-specific stimuli. PF-04957325 increased 1 nM isoproterenol–stimulated cAMP responses in a concentration-dependent manner (Figures 5B and 5D). PF-04957325 effects on the rate of isoproterenol-stimulated cAMP production (expressed as the rate constant, *k*, of the decay of the fluorescent cADDis sensor) appeared to have both low-affinity and high-affinity components (Figure 5D, black bars). The decrease in cAMP concentrations at 10 nM PF-04957325 may be due to PKA-mediated phosphorylation of PDE8 that enhances its activity or to inhibition of other PDE isoforms by higher concentrations of PF-04957325 (37). cAMP production by 3 nM PGE_2 stimulation was not enhanced by any concentration of PF-04957325 (Figures 5C and 5D). PF-04957325 did not increase cAMP signaling in conditions with preferential activation of either EP_2Rs or EP_4Rs (*see* Figure E2 in the data supplement). Thus, PDE8 activity specifically regulates cAMP signals generated by β_2AR without significant effects on cAMP stimulated by either EP_2R or EP_4R.

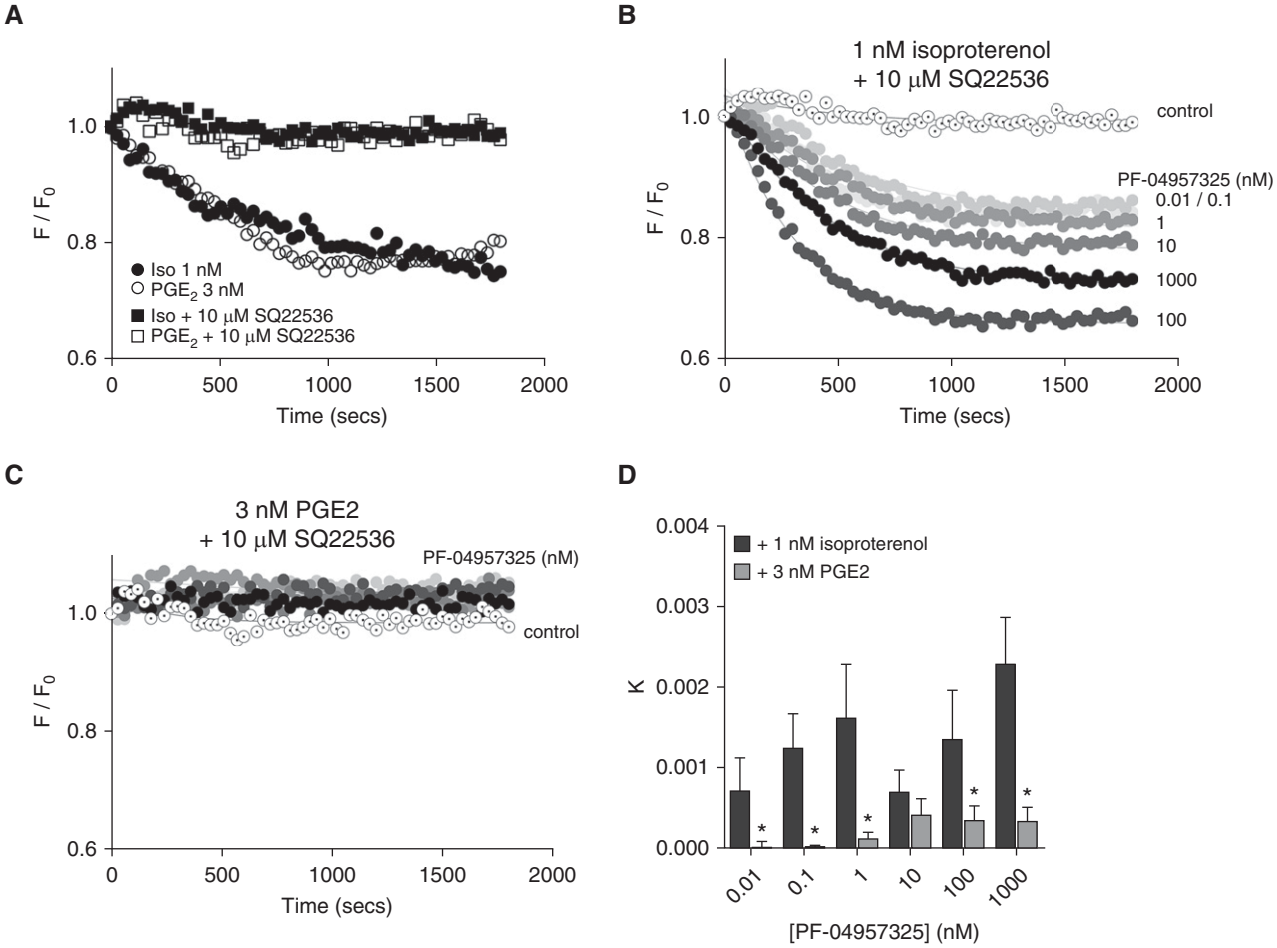

Figure 5. Dose response of the selective PDE8 inhibitor PF-04957325 on isoproterenol- or prostaglandin E_2 (PGE_2)-stimulated cAMP dynamics in live HASM cells. (*A*) Representative cAMP difference detector *in situ* sensor fluorescence decay curves (F/F_0) are shown for minimally effective concentrations of isoproterenol (1 nM) or PGE_2 (3 nM) with and without 10 μM SQ22536 to suppress basal adenylyl cyclase activity. Various concentrations of PF-04957325 were then added to these same conditions. Representative decay curves are shown in the presence of 10 μM SQ22536 plus either (*B*) 1 nM isoproterenol or (*C*) 3 nM PGE_2. PF-04957325 was tested at concentrations from 10^{-11} M (lightest circle) to 10^{-6} M (black circle). (*D*) Kinetic rate constants (*k*) from one-phase decay analysis (with a shared constrained plateau) were calculated for each dose of PF-04957325, and the pooled data from multiple experiments is shown. Each bar represents the mean ± SEM ($n = 5$ experiments). *$P < 0.05$ by paired *t* test as compared with isoproterenol.

On the basis of the fact that PDE8A selectively regulated β_2AR- and AC6-mediated cAMP production, we hypothesized that it is localized in lipid raft microdomains. PDE8A has been reported in detergent-resistant membranes from mural granulosa cells, but the researchers in the reported study did not use sucrose density centrifugation to isolate lipid rafts (39). We used a nondetergent method followed by sucrose gradient centrifugation to isolate lipid raft fractions from control HASM cells. We have previously reported that β_2AR, natively expressed AC6, and overexpressed AC6 colocalize in lipid raft domains, but that EP_2R, EP_4R, and AC2 are excluded from these domains (8, 9). Immunoblot analysis of these fractions indicates that PDE8A colocalizes with natively expressed caveolin-1 and AC6 in buoyant lipid raft fractions numbered 3–5, but not in fractions 6–10 associated with nonraft membranes and the bulk of the cellular material (Figure 6). AC2

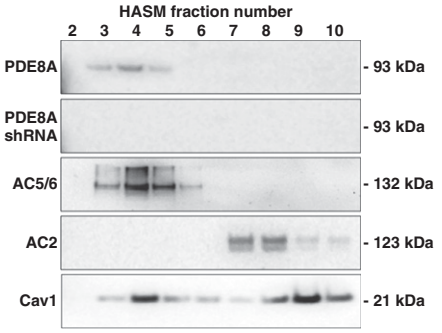

Figure 6. Western blot analysis of PDE8A in fractions derived from sucrose density centrifugation of control HASM cells or cells incubated 72 hours with recombinant lentivirus-expressing PDE8A shRNA. Cells were fractionated using a nondetergent method and separated by sucrose density centrifugation (*see* METHODS section of main text). Gradients were collected in ten 0.5-ml fractions, separated by SDS-PAGE, and analyzed by immunoblotting using a primary antibody for PDE8A. Fractions were also probed for native expression of AC6, AC2, and caveolin-1 (Cav1) using antibodies for AC5/6, AC2, and Cav1 to show appropriate fractionation. Both control and PDE8A-knockdown HASM cells displayed similar distributions of Cav1, AC5/6, and AC2. Fractions 3–5 contain buoyant lipid raft membranes, whereas fractions 6–10 contain the rest of the cellular material. Shown are regions of the gels at the approximate molecular weight of the expected immunoreactive band. Images shown are representative of three experiments.

immunoreactivity was detected only in lower fractions associated with non–lipid raft membranes and other cellular organelles. HASM cells incubated with lentivirus-expressing PDE8A shRNA displayed no PDE8A immunoreactive bands near 93 kD after fractionation. These data are consistent with the idea that PDE8A localizes in lipid raft microdomains, where it selectively regulates signaling by β_2AR and AC6.

β_2AR agonists and other cAMP-elevating agents inhibit serum- and growth factor–stimulated cell proliferation (40). We examined the effects of PF-04957325 on cell proliferation stimulated by serum. After 48 hours of serum starvation, HASM cells were incubated with 10% FBS and either PF-04957325 (1 μM), isoproterenol (1 μM), or PF-04957325 plus isoproterenol. PF-04957325, isoproterenol, or their combination did not significantly alter cell proliferation in the absence of FBS (Figure 7A). FBS stimulated cell proliferation nearly threefold, and treatment with just 1 μM isoproterenol or 1 μM PF-04957325 did not inhibit this response. We chose a submaximal concentration of isoproterenol for this study so that any additive effect from inhibition of PDE activity could be observed. Indeed, treatment of HASM cells with both isoproterenol and PF-04957325 significantly inhibited cell proliferation compared with FBS alone ($P < 0.01$ by paired *t* test). We also examined the effect of PGE_2 on HASM cell proliferation. PGE_2 at 1 μM induced a small but significant ($P < 0.05$) inhibition of FBS-stimulated cell proliferation, but adding PF-04957325 did not increase this effect (Figure 7B). Therefore, inhibition of PDE8 activity increases the ability of β_2AR to regulate cell proliferation, but it has no effect on PGE_2-mediated regulation of cell proliferation.

Discussion

PDE8 function has previously been ascribed to roles in T-cell adhesion (37), adrenal (41, 42) and Leydig cell steroidogenesis (32, 43), heartbeat regulation (24), and lymphocyte/breast cancer chemotaxis (44, 45). We report the transcript, protein, and functional presence of PDE8 in HASM cells. Our transcriptomic data demonstrate the presence of all PDE isoenzymes, except PDE2, via selective expression of 18 of 24 PDE genes in HASM cells derived from donors with asthma and fatal asthma. Previously, studies were focused on soluble inhibitors to characterize PDE function in HASM cells (18). We hypothesized that PDE8 was functionally relevant in HASM cells because dipyridamole, a semiselective PDE5/8 inhibitor (22), induced small but nonsignificant increases in forskolin-stimulated cAMP accumulation (Figure 2A). Dipyridamole enhanced forskolin-stimulated cAMP production in HASM cells overexpressing AC6, but not in cells overexpressing AC2, implying that PDE8 may selectively regulate signaling in AC6 microdomains. These initial results with dipyridamole were supported by knockdown of *PDE8A* expression with shRNA. *PDE8A* knockdown selectively enhanced cAMP production in AC6-overexpressing cells relative to AC2 in basal and forskolin-stimulated conditions (Figures 3B and 3C). Moreover, knockdown of PDE8 expression shifts the forskolin dose–response curve to a higher maximum in AC6-overexpressing cells (Figure 3E), but not when AC2 was overexpressed (Figure 3D). These results indicate that PDE8 changes the gain of local cAMP signaling so that stimulation of AC causes a proportionally stronger response in this particular cAMP microdomain.

Measuring cAMP concentrations in the presence of IBMX does not allow the interpretation of the relative importance of PDE8 in cAMP signaling compared with other PDE isoforms. Therefore, we sought an assay capable of sensitively detecting cAMP concentrations without broad PDE inhibition. Expression of the "downward" cADDis cAMP sensor allows sensitive detection of intracellular cAMP kinetics in live cells without PDE inhibition (Figures 4A and 4C) (36). We initially determined that lentiviral infection of HASM cells reduces baculovirus modified with a mammalian promoter infection and expression of the cADDis cAMP sensor. Therefore, shRNA knockdown of PDE8 is not compatible with the cADDis assay using the methods we employed. Instead, we employed the PDE8-selective inhibitor PF-04957325 (42). PF-04957325 dose dependently enhanced the rate constant (*k*) for cAMP formation in the absence of any GPCR agonist or AC activator, indicating that accumulation of cAMP was accelerated. The response to PF-04957325 was concentration dependent and nearly

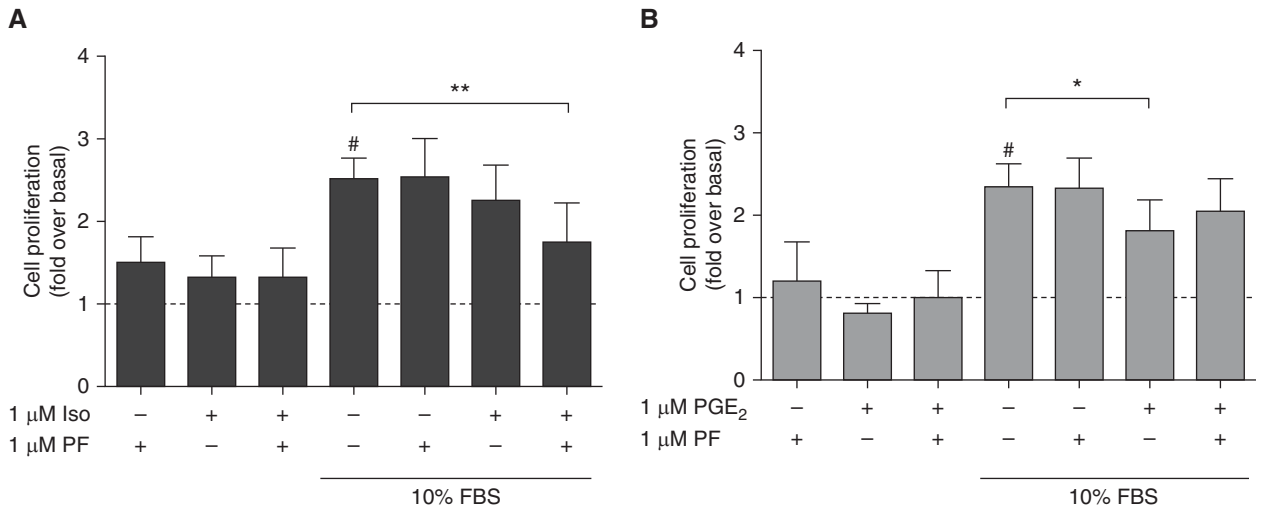

Figure 7. Cell proliferation was measured using the CyQUANT NF Cell Proliferation Assay Kit with HASM cells stimulated with 10% FBS for 48 hours. (*A*) Isoproterenol (Iso; 1 μM) or (*B*) PGE_2 was included with and without addition of 1 μM PF-04957325 (PF) in both serum-free and 10% FBS conditions. The data are normalized to the serum-free basal condition and expressed as fold change over basal levels. Each bar represents the mean ± SEM ($n = 4$–7 experiments). $^{\#}P < 0.05$ as compared with serum-free basal condition; $^{*}P < 0.05$ and $^{**}P < 0.01$ as compared with 10% FBS alone by paired *t* test.

as efficacious as forskolin (Figure 4A), and it was more efficacious than the response to the PDE4 inhibitor rolipram (Figure 4C). Thus, basal cAMP signaling within HASM cells appears to be at least partly under PDE8 control.

We next examined the effect of PDE8 inhibition on small cAMP responses that were directly attributable to either isoproterenol or PGE_2. Addition of PF-04957325 increased cAMP concentrations in the presence of isoproterenol but had no effect (in fact slightly inhibited) responses in the presence of PGE_2 (Figures 5A and 5B). These responses were accompanied by selective changes in the rate constant (*k*) of cAMP formation in isoproterenol-stimulated responses but not PGE_2-stimulated responses (Figure 5C). Interestingly, the effects of PF-04957325 on isoproterenol-induced responses appeared to have both high-affinity and low-affinity components (Figures 4C and 5C). The reason for this is unknown, but it might be related to PKA activation of PDE8 activity as cAMP concentrations increase or to inhibition of other PDE isoforms at higher concentrations of PF-04657325. Nonetheless, functionally responsive PDE8 appears in β_2AR but not EP_2R signaling microdomains.

We have previously established that β_2ARs are colocalized in lipid raft fractions with AC5/6, whereas AC2 is localized in nonraft fractions, where it is colocalized with $EP_{2/4}$R (9). This is evident in HASM cells as well as many other cells and tissues (46, 47). We now show that PDE8A immunoreactivity is similarly localized in lipid raft fractions of HASM cells. (PDE8 shRNA knockdown eliminated this signal; *see* Figure 6.) The selective effect of PDE8 in regulating cAMP concentrations in the β_2AR compartment is also evident at the functional level. Examination of cell proliferation regulated by both PGE_2 and isoproterenol with and without the PDE8-selective inhibitor makes it clear that PDE8 activity regulates signaling by β_2ARs but has no effect on PGE_2-mediated signaling (Figure 7) through either EP_2Rs or EP_4Rs (Figure E2). Taken together, our data indicate that PDE8 colocalizes with β_2AR-AC6 in lipid raft microdomains and shapes cAMP signals and cellular responses to β_2ARs. We speculate that PDE8 provides a highly localized regional brake on cAMP signaling in HASM cells so that low threshold activation of signaling in this compartment is suppressed to minimize indiscriminate recruitment of downstream signaling effectors. The exact role of PDE8 and its regulation of β_2AR-AC6 signaling could be to regulate cell shape, proliferation, contractility, or perhaps overall responsiveness to changes in parasympathetic tone or other relevant hormones in the blood as a way to manage resting versus active metabolic demands (48, 49).

The utility of modulating PDEs for treatment of lung disorders such as asthma and COPD has been evaluated extensively in clinical research and has culminated with the approval of roflumilast, a PDE4 inhibitor, for treatment of severe COPD (18). However, PDE4-selective inhibitors exhibit a therapeutic window that is too narrow for wider use, owing to target-related gastrointestinal side effects such as nausea, vomiting, diarrhea, abdominal pain, and dyspepsia. Strategies to mitigate side effects have included combined PDE3/4 inhibition because PDE3 inhibition can synergize with PDE4 in lung bronchoconstriction and inflammation (50, 51). In addition to possible cardiac side effects, this particular strategy may be confounded by metabolic dysregulation leading to insulin resistance, as seen in $PDE3B^{-/-}$ knockout animals (52). Moreover, several PDE3/4 dual inhibitors in clinical development have been discontinued, indicating that the potential synergy is not sufficient to widen the therapeutic window significantly. Although the concept of modulating cAMP-sensitive pathways via inhibition of PDE activity remains attractive, more selective means of achieving signal control are needed (18). Perhaps modulation of PDE8 enzymes within HASM could be a selective means for altering cellular responses associated with asthma or COPD, especially in the context of using agonists for β_2ARs or other GPCRs as cotherapies (53). For example, compartment-specific, basal cAMP-directed

effects of PDE8 that occur in HASM cells could be a relevant target for subtle modulation of β_2AR-induced bronchodilation without long-term desensitization, increases in smooth muscle hypertrophy, or enhancement of cAMP signaling by other signals, such as prostaglandins.

To our knowledge, our present data are the first to demonstrate PDE8 expression and function in ASM. We show that it regulates cAMP signaling stimulated by β_2ARs but does not alter prostaglandin-stimulated cAMP concentrations in HASM cells. Although more studies are needed to characterize the role of PDE8 in regulating human bronchodilation, it is clear that this unique PDE isoform has potential as a therapeutic target in asthma and COPD. ■

Author disclosures are available with the text of this article at www.atsjournals.org.

Acknowledgment: The authors thank Drs. Raymond Penn and Tonio Pera, Thomas Jefferson University, and Drs. Gaoyuan Cao and Brian Deeney, Rutgers University, for isolating and providing HASM cells. PF-04957325 was a generous gift of Pfizer, Inc.

References

1. Morgan SJ, Deshpande DA, Tiegs BC, Misior AM, Yan H, Hershfeld AV, *et al*. β-Agonist-mediated relaxation of airway smooth muscle is protein kinase A-dependent. *J Biol Chem* 2014;289:23065–23074.
2. Baillie GS. Compartmentalized signalling: spatial regulation of cAMP by the action of compartmentalized phosphodiesterases. *FEBS J* 2009; 276:1790–1799.
3. Houslay MD. Underpinning compartmentalised cAMP signalling through targeted cAMP breakdown. *Trends Biochem Sci* 2010;35:91–100.
4. Ostrom RS, Bogard AS, Gros R, Feldman RD. Choreographing the adenylyl cyclase signalosome: sorting out the partners and the steps. *Naunyn Schmiedebergs Arch Pharmacol* 2012;385:5–12.
5. May DC, Ross EM, Gilman AG, Smigel MD. Reconstitution of catecholamine-stimulated adenylate cyclase activity using three purified proteins. *J Biol Chem* 1985;260:15829–15833.
6. Taussig R, Iñiguez-Lluhi JA, Gilman AG. Inhibition of adenylyl cyclase by Gi alpha. *Science* 1993;261:218–221.
7. Cooper DM, Tabbasum VG. Adenylate cyclase-centred microdomains. *Biochem J* 2014;462:199–213.
8. Bogard AS, Xu C, Ostrom RS. Human bronchial smooth muscle cells express adenylyl cyclase isoforms 2, 4, and 6 in distinct membrane microdomains. *J Pharmacol Exp Ther* 2011;337:209–217.
9. Bogard AS, Adris P, Ostrom RS. Adenylyl cyclase 2 selectively couples to E prostanoid type 2 receptors, whereas adenylyl cyclase 3 is not receptor-regulated in airway smooth muscle. *J Pharmacol Exp Ther* 2012;342:586–595.
10. Bogard AS, Birg AV, Ostrom RS. Non-raft adenylyl cyclase 2 defines a cAMP signaling compartment that selectively regulates IL-6 expression in airway smooth muscle cells: differential regulation of gene expression by AC isoforms. *Naunyn Schmiedebergs Arch Pharmacol* 2014;387:329–339.
11. Agarwal SR, Miyashiro K, Latt H, Ostrom RS, Harvey RD. Compartmentalized cAMP responses to prostaglandin EP2 receptor activation in human airway smooth muscle cells. *Br J Pharmacol* 2017;174:2784–2796.
12. Zaccolo M. Spatial control of cAMP signalling in health and disease. *Curr Opin Pharmacol* 2011;11:649–655.
13. Manning CD, McLaughlin MM, Livi GP, Cieslinski LB, Torphy TJ, Barnette MS. Prolonged β adrenoceptor stimulation up-regulates cAMP phosphodiesterase activity in human monocytes by increasing mRNA and protein for phosphodiesterases 4A and 4B. *J Pharmacol Exp Ther* 1996;276:810–818.
14. Seybold J, Newton R, Wright L, Finney PA, Suttorp N, Barnes PJ, *et al*. Induction of phosphodiesterases 3B, 4A4, 4D1, 4D2, and 4D3 in Jurkat T-cells and in human peripheral blood T-lymphocytes by 8-bromo-cAMP and G_s-coupled receptor agonists: potential role in β_2-adrenoreceptor desensitization. *J Biol Chem* 1998;273: 20575–20588.
15. Dodge KL, Khouangsathiene S, Kapiloff MS, Mouton R, Hill EV, Houslay MD, *et al*. mAKAP assembles a protein kinase A/PDE4 phosphodiesterase cAMP signaling module. *EMBO J* 2001;20: 1921–1930.
16. Horvat SJ, Deshpande DA, Yan H, Panettieri RA, Codina J, DuBose TD Jr, *et al*. A-kinase anchoring proteins regulate compartmentalized cAMP signaling in airway smooth muscle. *FASEB J* 2012;26: 3670–3679.
17. Hu A, Nino G, Grunstein JS, Fatma S, Grunstein MM. Prolonged heterologous β_2-adrenoceptor desensitization promotes proasthmatic airway smooth muscle function via PKA/ERK1/2-mediated phosphodiesterase-4 induction. *Am J Physiol Lung Cell Mol Physiol* 2008;294:L1055–L1067.
18. Page CP. Phosphodiesterase inhibitors for the treatment of asthma and chronic obstructive pulmonary disease. *Int Arch Allergy Immunol* 2014;165:152–164.
19. Lynch MJ, Baillie GS, Houslay MD. cAMP-specific phosphodiesterase-4D5 (PDE4D5) provides a paradigm for understanding the unique non-redundant roles that PDE4 isoforms play in shaping compartmentalized cAMP cell signalling. *Biochem Soc Trans* 2007; 35:938–941.
20. Kokkonen K, Kass DA. Nanodomain regulation of cardiac cyclic nucleotide signaling by phosphodiesterases. *Annu Rev Pharmacol Toxicol* 2017;57:455–479.
21. Maurice DH, Ke H, Ahmad F, Wang Y, Chung J, Manganiello VC. Advances in targeting cyclic nucleotide phosphodiesterases. *Nat Rev Drug Discov* 2014;13:290–314.
22. Soderling SH, Bayuga SJ, Beavo JA. Cloning and characterization of a cAMP-specific cyclic nucleotide phosphodiesterase. *Proc Natl Acad Sci USA* 1998;95:8991–8996.
23. Wang H, Yan Z, Yang S, Cai J, Robinson H, Ke H. Kinetic and structural studies of phosphodiesterase-8A and implication on the inhibitor selectivity. *Biochemistry* 2008;47:12760–12768.
24. Patrucco E, Albergine MS, Santana LF, Beavo JA. Phosphodiesterase 8A (PDE8A) regulates excitation-contraction coupling in ventricular myocytes. *J Mol Cell Cardiol* 2010;49:330–333.
25. Hill KM, Li F, Bogard AS, Ostrom RS. The IBMX-insensitive PDE8A is expressed in human airway smooth muscle cells and selectively regulates signaling through AC6 [abstract]. *FASEB J* 2016;30(1, Suppl):1190.8.
26. Panettieri RA, Murray RK, DePalo LR, Yadvish PA, Kotlikoff MI. A human airway smooth muscle cell line that retains physiological responsiveness. *Am J Physiol* 1989;256:C329–C335.
27. Himes BE, Koziol-White C, Johnson M, Nikolos C, Jester W, Klanderman B, *et al*. Vitamin D modulates expression of the airway smooth muscle transcriptome in fatal asthma. *PLoS One* 2015;10: e0134057.
28. Cooper PR, Mesaros AC, Zhang J, Christmas P, Stark CM, Douaidy K, *et al*. 20-HETE mediates ozone-induced, neutrophil-independent airway hyper-responsiveness in mice. *PLoS One* 2010;5:e10235.
29. Bolger AM, Lohse M, Usadel B. Trimmomatic: a flexible trimmer for Illumina sequence data. *Bioinformatics* 2014;30:2114–2120.
30. Bray NL, Pimentel H, Melsted P, Pachter L. Near-optimal probabilistic RNA-seq quantification. *Nat Biotechnol* 2016;34:525–527.
31. Pimentel H, Bray NL, Puente S, Melsted P, Pachter L. Differential analysis of RNA-seq incorporating quantification uncertainty. *Nat Methods* 2017;14:687–690.
32. Vasta V, Shimizu-Albergine M, Beavo JA. Modulation of Leydig cell function by cyclic nucleotide phosphodiesterase 8A. *Proc Natl Acad Sci USA* 2006;103:19925–19930.
33. Soderling SH, Beavo JA. Regulation of cAMP and cGMP signaling: new phosphodiesterases and new functions. *Curr Opin Cell Biol* 2000;12: 174–179.
34. Francis SH, Sekhar KR, Ke H, Corbin JD. Inhibition of cyclic nucleotide phosphodiesterases by methylxanthines and related compounds. *Handb Exp Pharmacol* 2011;(200):93–133.

35. van Aubel RA, Smeets PH, Peters JG, Bindels RJ, Russel FG. The MRP4/ABCC4 gene encodes a novel apical organic anion transporter in human kidney proximal tubules: putative efflux pump for urinary cAMP and cGMP. *J Am Soc Nephrol* 2002;13:595–603.
36. Tewson PH, Martinka S, Shaner NC, Hughes TE, Quinn AM. New dag and camp sensors optimized for live-cell assays in automated laboratories. *J Biomol Screen* 2016;21:298–305.
37. Vang AG, Ben-Sasson SZ, Dong H, Kream B, DeNinno MP, Claffey MM, *et al*. PDE8 regulates rapid Teff cell adhesion and proliferation independent of ICER. *PLoS One* 2010;5:e12011.
38. Emery AC, Eiden MV, Eiden LE. A new site and mechanism of action for the widely used adenylate cyclase inhibitor SQ22,536. *Mol Pharmacol* 2013;83:95–105.
39. Bergeron A, Guillemette C, Sirard MA, Richard FJ. Active 3′-5′ cyclic nucleotide phosphodiesterases are present in detergent-resistant membranes of mural granulosa cells. *Reprod Fertil Dev* 2017;29:778–790.
40. Kassel KM, Wyatt TA, Panettieri RA Jr, Toews ML. Inhibition of human airway smooth muscle cell proliferation by β_2-adrenergic receptors and cAMP is PKA independent: evidence for EPAC involvement. *Am J Physiol Lung Cell Mol Physiol* 2008;294:L131–L138.
41. Tsai LC, Beavo JA. Regulation of adrenal steroidogenesis by the high-affinity phosphodiesterase 8 family. *Horm Metab Res* 2012;44:790–794.
42. Tsai LC, Shimizu-Albergine M, Beavo JA. The high-affinity cAMP-specific phosphodiesterase 8B controls steroidogenesis in the mouse adrenal gland. *Mol Pharmacol* 2011;79:639–648.
43. Shimizu-Albergine M, Tsai LC, Patrucco E, Beavo JA. cAMP-specific phosphodiesterases 8A and 8B, essential regulators of Leydig cell steroidogenesis. *Mol Pharmacol* 2012;81:556–566.
44. Dong H, Osmanova V, Epstein PM, Brocke S. Phosphodiesterase 8 (PDE8) regulates chemotaxis of activated lymphocytes. *Biochem Biophys Res Commun* 2006;345:713–719.
45. Dong H, Claffey KP, Brocke S, Epstein PM. Inhibition of breast cancer cell migration by activation of cAMP signaling. *Breast Cancer Res Treat* 2015;152:17–28.
46. Dessauer CW, Watts VJ, Ostrom RS, Conti M, Dove S, Seifert R. International Union of Basic and Clinical Pharmacology. CI. Structures and small molecule modulators of mammalian adenylyl cyclases. *Pharmacol Rev* 2017;69:93–139.
47. Ostrom RS, Insel PA. The evolving role of lipid rafts and caveolae in G protein-coupled receptor signaling: implications for molecular pharmacology. *Br J Pharmacol* 2004;143:235–245.
48. Brown KM, Day JP, Huston E, Zimmermann B, Hampel K, Christian F, *et al*. Phosphodiesterase-8A binds to and regulates Raf-1 kinase. *Proc Natl Acad Sci USA* 2013;110:E1533–E1542.
49. Cao L, Zhang Y, Cao YX, Edvinsson L, Xu CB. Secondhand smoke exposure causes bronchial hyperreactivity via transcriptionally upregulated endothelin and 5-hydroxytryptamine 2A receptors. *PLoS One* 2012;7:e44170.
50. Franciosi LG, Diamant Z, Banner KH, Zuiker R, Morelli N, Kamerling IM, *et al*. Efficacy and safety of RPL554, a dual PDE3 and PDE4 inhibitor, in healthy volunteers and in patients with asthma or chronic obstructive pulmonary disease: findings from four clinical trials. *Lancet Respir Med* 2013;1:714–727.
51. Wedzicha JA. Dual PDE 3/4 inhibition: a novel approach to airway disease? *Lancet Respir Med* 2013;1:669–670.
52. Choi YH, Park S, Hockman S, Zmuda-Trzebiatowska E, Svennelid F, Haluzik M, *et al*. Alterations in regulation of energy homeostasis in cyclic nucleotide phosphodiesterase 3B-null mice. *J Clin Invest* 2006;116:3240–3251.
53. Penn RB, Benovic JL. Regulation of heterotrimeric G protein signaling in airway smooth muscle. *Proc Am Thorac Soc* 2008;5:47–57.